Available online at www.sciencedirect.com
ScienceDirect
Journal of Natural Gas Chemistry 20(2011)477–482
JOURNAL OF NATURAL GAS CHEMISTRY
www.elsevier.com/locate/jngc

# Effect of iridium loading on HZSM-5 for isomerization of $n$-heptane

Herma Dina Setiabudi[1], Sugeng Triwahyono[2*], Aishah Abdul Jalil[1], Nur Hidayatul Nazirah Kamarudin[1], Muhammad Arif Ab Aziz[1]

*1. Department of Chemical Engineering, Faculty of Chemical Engineering, Universiti Teknologi Malaysia, 81310 UTM Johor Bahru, Johor, Malaysia;*
*2. Ibnu Sina Institute for Fundamental Science Studies, Faculty of Science, Universiti Teknologi Malaysia, 81310 UTM Johor Bahru, Johor, Malaysia*

[ Manuscript received April 29, 2011; revised June 7, 2011 ]

**Abstract**
The effect of iridium loading on the properties and catalytic isomerization of $n$-heptane over Ir-HZSM-5 is studied. Ir-HZSM-5 was prepared by impregnation method and subjected to isomerization process in the presence of flowing hydrogen gas. XRD and BET studies show that the presence of iridium stabilizes the crystalline structure of HZSM-5, leading to more ordered framework structure and larger surface area. TGA and FTIR results substantiate that iridium species interacts with OH group on the surface of HZSM-5. Pyridine FT-IR study verifies the interaction between iridium and surface OH group slightly increased the Brönsted and Lewis acid sites without changing the lattice structure of HZSM-5. The presence of iridium and the increase of strong Lewis acid sites on HZSM-5 were found to bring an increase about 4.1%, 33.2% and 11.8% in conversion, selectivity and yield of $n$-heptane isomerization, respectively.

**Key words**
Ir-HZSM-5; *n*-heptane isomerization; Lewis acid sites; protonic acid sites

## 1. Introduction

Recently, the increasing environmental awareness has led to strong restrictions on gasoline contents in aromatic compounds. This has caused oil refineries to continuously reformulate their gasoline composition in an attempt to keep their product quality while minimize adverse effects to men and the environment. As a result, there is a need to maintain the number of available octane, which has recently attracted much interest in isomerization process involving alkanes, particularly linear chain alkanes. Many studies show that transition metal or noble metal loaded on metal oxide [1−8], mesoporous [9,10] or microporous [11−14] materials possesses high activity for the isomerization of linear chain alkanes. Among those supports, zeolite provides an effective choice for the isomerization process owing to their large surface area, high thermal stability and resistance towards coke formation. In the field of zeolite, HZSM-5 is most extensively used due to its shape-selective properties of medium pore-size, high thermal stability and high acidity which are prerequisites for application in isomerization reaction.

It is noteworthy that the activity and selectivity of the zeolite are significantly influenced by the presence of metal. Particularly, among the noble metals present in nature, only platinum, palladium and iridium have high potential to be a good catalyst in isomerization of $n$-alkanes [15,16]. It has been reported by several researchers that HZSM-5 zeolite modified with platinum [11,17] and palladium [18] is able to increase the activity and selectivity of the catalyst rather than cracking. However, only a few publications concerning the isomerization of $n$-alkanes over Ir catalyst loaded on zeolite were reported, even though iridium species is one of the well-known promoters of catalyst due to its activity towards isomerization [19] and its stability effect through the removal of coke-precursor [20]. Yang and Woo [21] reported that Ir/NaY showed higher conversion and stability than Pt/NaY catalyst towards $n$-heptane reforming reaction because of the high activity of hydrogenolysis reaction which resulted in less amount of coke on the Ir/NaY surface.

In addition, detailed study of the properties particularly structural properties and nature of acidity of iridium loaded on zeolite has not yet been clearly reported. Therefore, in the present paper, we reported the properties of Ir-HZSM-5 catalyst and also its activity towards isomerization of $n$-heptane.

* Corresponding author. Tel: +60-7-5536076; Fax: +60-7-5536080; E-mail: sugeng@utm.my; aishah@cheme.utm.my
This work was supported by the Ministry of Science, Technology and Innovation, Malaysia through E-Science Fund Research Project (No. 03-01-06-SF0564 and 03-01-06-SF0289), and the Hitachi Scholarship Foundation for the Gas Chromatograph Instrument Grant.


doi:10.1016/S1003-9953(10)60227-7

For this purpose, XRD, BET, TGA and FT-IR measurements were employed to observe the structural properties of the catalyst, and the adsorption of pyridine as a probe molecule was also performed to identify the acidity nature of the catalyst.

## 2. Experimental

### 2.1. Catalyst preparation

A commercial HZSM-5 (Zeolyst) was used as a catalyst support. Ir-HZSM-5 was prepared by incipient wetness impregnation of HZSM-5 with aqueous solution of $IrCl_3 \cdot 3H_2O$ (Merck) followed by drying at 383 K overnight and calcination at 823 K for 3 h in air. The content of Ir was 0.1 wt%.

### 2.2. Catalyst characterization

The crystalline structure of the sample was determined with X-ray diffraction (XRD) recorded on a Bruker AXS D8 automatic powder diffractometer using Cu $K_\alpha$ radiation with $\lambda$ = 1.5418 Å at 40 kV and 40 mA in the range of $2\theta = 2^o - 22^o$.

The BET surface area and total pore volume of the sample were determined by $N_2$ adsorption-desorption isotherm using a Quantachrome Autosorb-1 at 77 K. Prior to the measurement, the sample was outgassed at 573 K for 3 h.

Thermogravimetric analysis (TGA) was conducted by the Mettler Toledo TGA/SDTA 851. Temperature was programmed from the ambient to 1173 K at a heating rate of 10 K/min under $N_2$ flow.

Fourier Transform Infra Red (FT-IR) measurements were carried out using Perkin-Elmer Spectrum GX FT-IR spectrometer. KBr pellet technique was used to determine the functional groups of catalyst. IR spectroscopy of adsorbed pyridine was used as a tool to evaluate the protonic and Lewis acid sites. The catalyst was activated before the analysis following the previously reported procedures [4]. A self-supported wafer placed in an in situ IR cell with $CaF_2$ windows was pretreated with hydrogen stream at 673 K, followed by outgassing at 673 K for 3 h. The measurement of pyridine adsorbed on the catalyst was conducted according to the method described in the literature [22]. The activated catalyst was exposed to 2 Torr of pyridine at 423 K followed by outgassing at 623 K for 15 min. The spectra were recorded at room temperature. In order to compare the surface coverage of the adsorbed species between different wafers, the overtone and combination vibrations of MFI between 2100 $cm^{-1}$ and 1550 $cm^{-1}$ after activation were used [23].

### 2.3. Catalyst testing

Isomerization of $n$-heptane was done in a microcatalytic pulse reactor at 623 K under hydrogen stream. 0.2 g catalyst was activated in oxygen stream for 1 h followed by hydrogen stream for 3 h at 673 K and then cooled down to 623 K in hydrogen stream. A dose of *n*-heptane was passed over the catalyst and the products were trapped at 77 K before flash-evaporated into the gas chromatograph. The reaction products were analysed by an on-line 6090N Agilent Gas Chromatograph equipped with HP-5 column and FID detector. The intervals between doses were kept constant at 20 min.

The selectivity to particular product ($S_i$) was calculated according to Equation (1)

$$S_i = \frac{A_i}{\sum A_i - A_{n\text{-heptane}}} \quad (1)$$

where $A_i$ is the corrected chromatographic area for particular compound. The conversion of $n$-heptane ($X_{n\text{-heptane}}$) was determined by Equation (2)

$$X_{n\text{-heptane}} = \frac{\sum A_i - A_{n\text{-heptane}}}{\sum A_i} \times 100 \quad (2)$$

The yield of $n$-heptane ($Y_{n\text{-heptane}}$) was determined by Equation (3).

$$Y_{n\text{-heptane}} = \frac{S_{iso\text{-heptane}} \times X_{n\text{-heptane}}}{100} \quad (3)$$

## 3. Results and discussion

### 3.1. Structural properties of HZSM-5 and Ir-HZSM-5

In order to determine the crystallinity of HZSM-5, the calibration curve of crystallinity against average peak intensity was plotted based on the physical mixture of pure $SiO_2$ and HZSM-5 in which the crystallinity of $SiO_2$ and HZSM-5 was assumed to be 0 and 100%, respectively. The XRD patterns of five samples with different HZSM/$SiO_2$ ratios are shown in Figure 1(a). Peaks in the range of $2\theta = 7^o - 10^o$ were identified as reflections of HZSM-5 zeolite [24]. No peak was observed at HZSM-5/$SiO_2$ ratio of 0 : 4, indicating that the sample was 0% in crystallinity. The intensities of the peaks of HZSM-5/$SiO_2$ reflections were increased significantly with the addition of HZSM-5. The calibration curve of HZSM-5 shown in Figure 1(b) was determined by comparing the average peak intensity of five samples. The calibration curve gave linear equation of $y = 2.14 \times 10^{-2} x$, where $y$ is the percentage of crystallinity and $x$ is the average peak intensity of the samples at $2\theta = 7.9^o$ and $8.9^o$.

Figure 2 shows the XRD pattern of HZSM-5 and Ir-HZSM-5. The introduction of iridium on HZSM-5 slightly increased the intensity of the peaks as well as the percentage of crystallinity of HZSM-5 from 100% to 103.4%. This result may indicate that iridium species induced the interaction with structural defect sites so as to stabilize the crystalline structure of HZSM-5 and led to more ordered framework structure. Generally, the introduction of metal species on zeolite support will change the intensity of the XRD peaks as well as the percentage of crystallinity of the support. Bhavani et al. [25] found that the addition of Ni into Pt-HY decreased the intensity of the XRD peaks which was caused by the pore blockage of support materials with Ni species. In contrast, Shen et al.

[26] reported that the addition of iridium into Fe-USY did not change the XRD pattern of Fe-USY, which can be ascribed to the well-controlled deposition of iridium to Fe-USY.

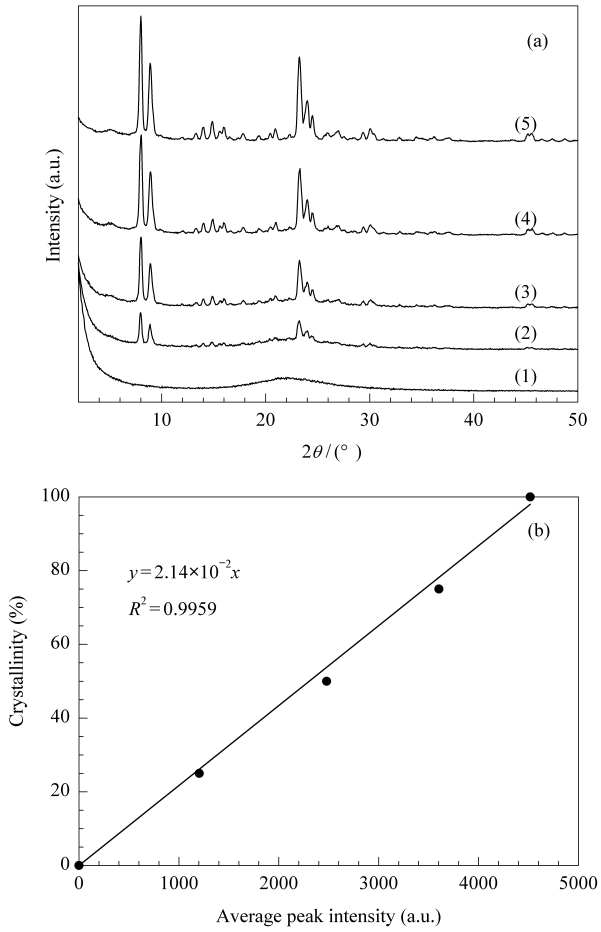


**Figure 1.** (a) XRD patterns of different samples with HZSM-5 : $SiO_2$ ratios of (1) 0 : 4, (2) 1 : 3, (3) 2 : 2, (4) 3 : 1 and (5) 4 : 0; (b) Calibration curve of the percentage of crystallinity against average peak intensity

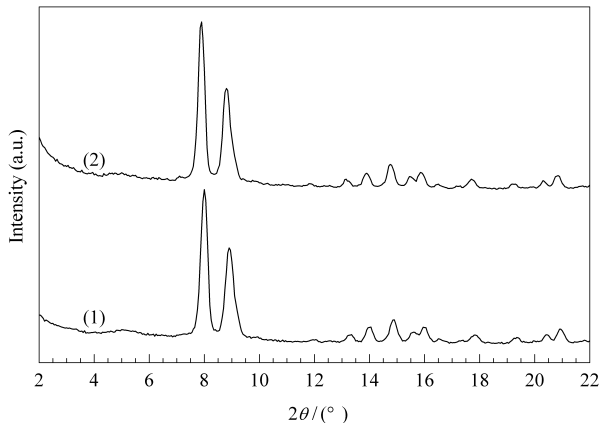


**Figure 2.** XRD patterns of HZSM-5 (1) and Ir-HZSM-5 (2)

The BET surface area and total pore volume of HZSM-5 and Ir-HZSM-5 are listed in Table 1. The small increase in the surface area and total pore volume of HZSM-5 may be related to small increase in the crystallinity of HZSM-5 by the introduction of Ir. The change of the textural properties of HZSM-5 zeolite caused by the introduction of metal species was also reported by de Lucas et al. [27] for molybdenum loaded on HZSM-5. They reported that the introduction of molybdenum prepared by impregnation method decreased the textural properties of HZSM-5, which can be attributed to partial blockage of the pore system caused mainly by the presence of metallic oxides and extra framework aluminum species localized in the interior of the pores and channels. In addition, M'Ramadj et al. [28] reported that the addition of CuO into HZSM-5 prepared by impregnating HZSM-5 with aqueous solution of copper nitrate decreased the BET surface area and total pore volume of the catalyst, which can be attributed to the blockage of a portion of the micropores in the catalyst with CuO species. In contrast, Shen et al. [26] reported that the BET surface area and total pore volume of Ir/Fe-USY were almost similar with those of Fe-USY, which indicated that the addition of iridium into Fe-USY does not change the textural properties of Fe-USY.

**Table 1. Structural properties of HZSM-5 and Ir-HZSM-5**

| Catalysts | XRD crystallinity (%) | BET surface area ($m^2/g$) | BET total pore volume ($cm^3/g$) |
|---|---|---|---|
| HZSM-5 | 100.0 | 437 | 0.27 |
| Ir-HZSM-5 | 103.4 | 458 | 0.39 |

Figure 3 shows the TGA curves of HZSM-5 and Ir-HZSM-5 catalysts. The TGA results explained the phenomenon of weight loss, which results from heating the samples in nitrogen flow. The curves for both catalysts showed a weight loss region in the range of 298 to 523 K, indicating the loss of zeolite water content. The weight loss percentages of HZSM-5 and Ir-HZSM-5 were about 8.60% and 7.94%, respectively. The introduction of iridium species slightly decreased the weight loss percentage may be due to the removal of OH groups by the interaction between iridium and HZSM-5 support, which was in agreement with the XRD results. In addition, none of the catalyst experienced the formation of

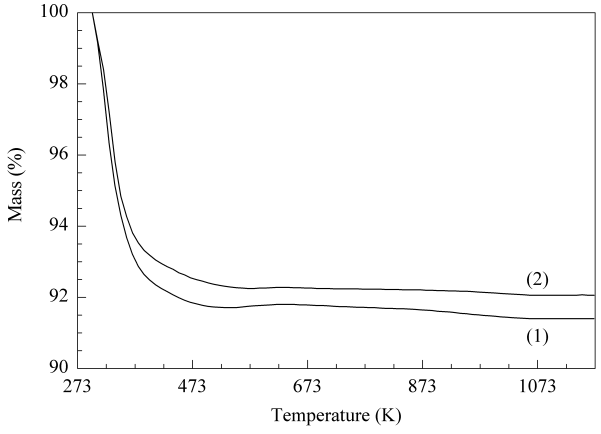


**Figure 3.** TGA curves of HZSM-5 (1) and Ir-HZSM-5 (2)

intermediate compound upon increasing the temperature. Similar result was observed on the vanadium loaded USY zeolite reported by Pérez et al. [29] in which the mass loss in the 589−635 K range was less pronounced when the zeolite contains vanadium.

Figure 4(a) shows the IR spectra of HZSM-5 and Ir-HZSM-5 in the region of 1600−400 $cm^{-1}$. The region of 1600−400 $cm^{-1}$ is attributed to the stretching and bending modes of the T−O units of the zeolite lattice. The most prominent band at 1250−950 $cm^{-1}$ is assigned to asymmetric stretching of intra-tetrahedral mode, while a weak band at 820−750 $cm^{-1}$ is assigned to symmetric stretching of inter-tetrahedral mode. The band at 650−500 $cm^{-1}$ is assigned to double ring of inter-tetrahedral mode, while the band at 500−420 $cm^{-1}$ is assigned to O−T−O bending of intra-tetrahedral mode [30]. The IR spectra of both catalysts were almost similar, indicating that the introduction of iridium does not change the lattice structure of HZSM-5.

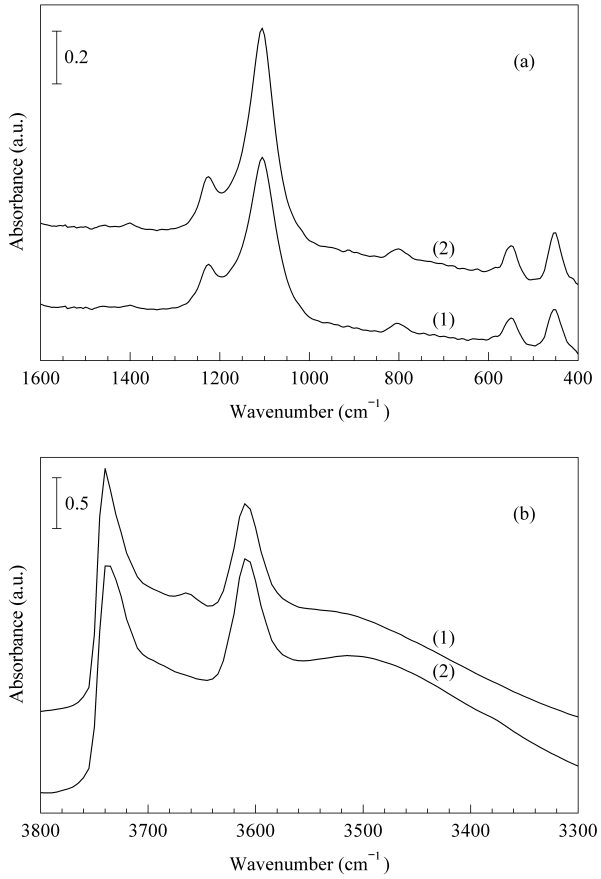


**Figure 4.** (a) FT-IR spectra of HZSM-5 (1) and Ir-HZSM-5 (2); (b) FT-IR spectra of activated Ir-HZSM-5 (1) and HZSM-5 (2)

The changes in the IR spectra of hydroxyl groups for both activated HZSM-5 and Ir-HZSM-5 catalysts are shown in Figure 4(b). There were four bands observed in this region. The narrow band at 3740 $cm^{-1}$ is assigned to the non acidic terminal silanol groups (Si−OH) located on the external surface of zeolite [30], while the shoulder band at approximately 3665 $cm^{-1}$ may be associated to the hydroxyl stretching on metal ion species [31,32]. A band at 3610 $cm^{-1}$ is assigned to the Brönsted hydroxyl associated with bridging hydroxyl groups (Si(OH)Al) located inside the zeolite structure, whereas the weak band at 3520 $cm^{-1}$ is associated to the perturbation of OH groups through the surrounding by lattice defects or extra lattice oxygen [30]. There is no change in the intensity of the band at 3740 $cm^{-1}$, indicating that non acidic terminal silanol groups does not interact with iridium. However, the presence of iridium led to a decrease in the intensity of the band at 3610 $cm^{-1}$ and developed a new band at 3665 $cm^{-1}$, indicating some exchange of isolated acidic hydroxyl groups with iridium cations. In addition, the band at 3520 $cm^{-1}$ decreased slightly with the addition of iridium. This may be due to the existence of iridium bonded to the framework of HZSM-5 through the surrounding by lattice defects or extra lattice oxygen.

The change of the ZSM-5 structure caused by the metal exchange was also observed on Fe loaded on ZSM-5 as reported by Guo et al. [33]. They reported that the introduction of Fe slightly decreased the intensity of the band at 3610 $cm^{-1}$ and developed a new band at 3670 $cm^{-1}$, in which the new band is assigned to the hydroxyl stretching on $Fe^{3+}$ species (Fe–OH). The reduction of the band at 3610 $cm^{-1}$ and the development of the new band at 3670 $cm^{-1}$ with the addition of Fe species indicated the displacement of Brönsted acid protons by Fe ions. Significant change of the structure was also observed on zirconia based catalyst in which the introduction of metal oxide, $WO_3$ on $ZrO_2$ developed the bands at 1021 $cm^{-1}$ and 1014 $cm^{-1}$. The band at 1021 $cm^{-1}$ is assigned to the stretching of the W=O which is connected to cus $Zr^{4+}$ through O, while the band at 1014 $cm^{-1}$ is assigned to the stretching of the W=O which is connected to the other W through O [34].

### *3.2. Acidic properties of HZSM-5 and Ir-HZSM-5*

The type of acid sites in HZSM-5 and Ir-HZSM-5 was qualitatively probed by pyridine molecule of which the adsorption was monitored by IR spectroscopy. Figure 5(a) shows the IR spectra of pyridine adsorbed on activated HZSM-5 and Ir-HZSM-5 at 423 K followed by heating in vacuum at 623 K. Since the catalysts were outgassed of 623 K after exposure to pyridine, the acid sites under consideration are only strong acid sites that can retain pyridine against outgassing temperature of 623 K and below. The band at 1545 $cm^{-1}$ is ascribed to pyridinium ions (pyridine adsorbed on protonic acid sites) and the band at 1445 $cm^{-1}$ is ascribed to pyridine adsorbed on Lewis acid sites. Both catalysts possessed strong protonic and Lewis acid sites, though the amount of protonic acid sites was dominant for both catalysts.

The amount of strong acid sites in HZSM-5 and Ir-HZSM-5 are more clearly seen in Figure 5(b), in which the absorbance of the bands at 1545 and 1445 $cm^{-1}$ are plotted in a bar chart. The introduction of iridium species influenced the acidic properties of HZSM-5 as well as the generation of small amount of protonic and Lewis acid sites, which may be

due to the interaction between iridium and lattice defects or extra-lattice oxygen. This result was inconsistent with that reported by Aboul-Gheit et al. [35] for Ir/HZSM-5 prepared by impregnation method of HZSM-5 with aqueous solution of $H_2IrCl_6{\cdot}6H_2O$ followed by drying at 110 °C and calcination in air at 530 °C for 3 h. The $NH_3$-TPD results showed that the addition of 0.35 wt% iridium to HZSM-5 slightly decreased the value of $\Delta H$ from 98.4 J/g to 87.5 J/g, indicating a small decrease of acid sites may be caused by the coverage of a portion of the acid sites with iridium. Similar phenomenon was also observed on iridium loaded on Mo/HZSM-5 in which the addition of 0.5 wt% iridium has caused a decrease of all the species of acid sites. In this report, iridium species effectively interacted with (or masked) a portion of the acid sites, thus decreased the amount of acid sites [36]. In previous work, we have reported that the impregnation of nano-Zn species into HZSM-5 eliminated weak and medium protonic acid sites and generated significant number of strong Lewis acid sites in which these Lewis acid sites provided by $Zn^{2+}$ cation exchanged in zeolite [37].

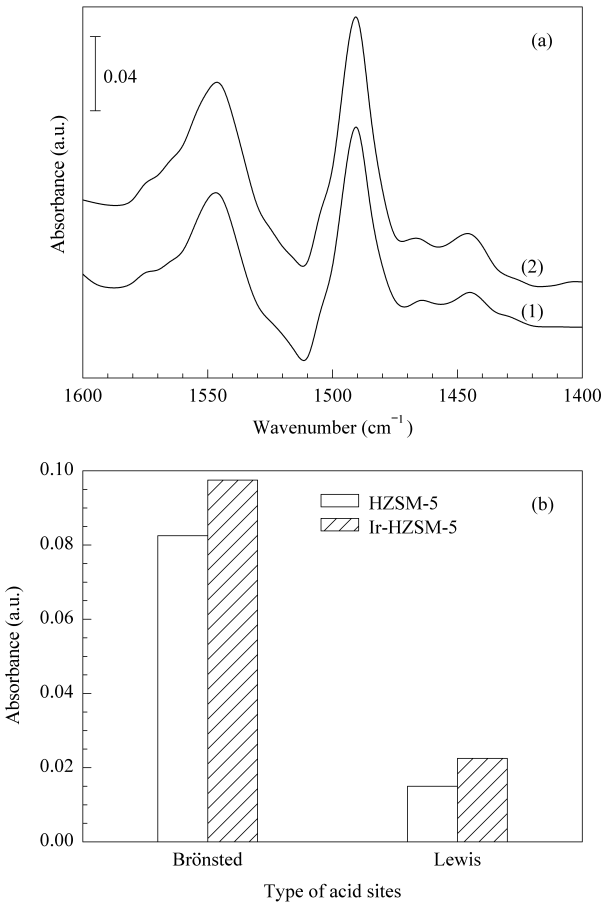


**Figure 5.** (a) IR spectra of pyridine adsorbed on activated catalysts at 423 K, followed by heating in the vacuum at 623 K for HZSM-5 (1) and Ir-HZSM-5 (2); (b) Absorbance of IR bands at Brönsted and Lewis acid sites for HZSM-5 and Ir-HZSM-5 after removal of pyridine at 623 K

The change of acidic nature caused by the introduction of metal on binary metal oxide was also observed on zirconia based catalysts. We have reported the addition of Pt into $WO_3$-$ZrO_2$ reduced protonic acid sites and generated Lewis acid sites [3]. In contrast, the introduction of sulfate ion generated strong acid sites and decreased the weak and medium acid sites due to the stabilization effect of sulfate ion on the metastable tetragonal phase of zirconia [4].

### 3.3. Isomerization of n-heptane

Figure 6 shows the isomerization of $n$-heptane over HZSM-5 and Ir-HZSM-5 catalysts at 623 K in a microcatalytic pulse reactor. The outlet was composed of $iso$-heptane, cracking-products ($C_1$–$C_6$) and residual $n$-heptane. The presence of iridium species resulted in a substantial increase in activity and selectivity to *iso*-heptane for *n*-heptance isomerization in the presence of hydrogen. The introduction of iridium into HZSM-5 catalyst increased about 4.1%, 33.2% and 11.8% in conversion, selectivity and yield of $n$-heptane isomerization, respectively. Whereas no activity was observed for the reaction in the absence of hydrogen (not shown). The increase in activity may be caused by the increase of the number of strong Lewis acid sites and the presence of iridium, which facilitated the formation of protonic acid sites through hydrogen spillover mechanism [3,38]. The iridium acts as a specific active site for dissociation-adsorption of molecular

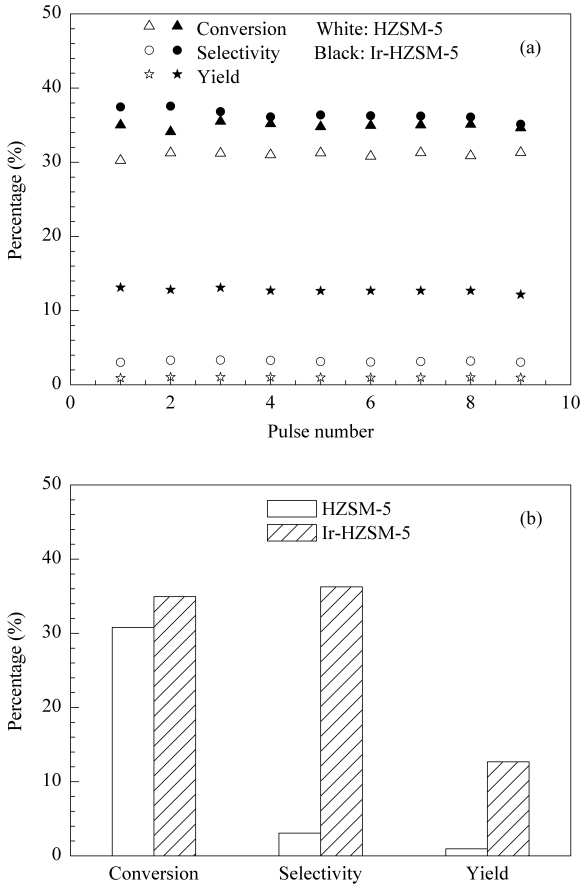


**Figure 6.** (a) Conversion, selectivity and yield of $n$-heptane isomerization over HZSM-5 and Ir-HZSM-5 at 623 K and different pulse numbers; (b) Conversion, selectivity and yield of $n$-heptane isomerization over HZSM-5 and Ir-HZSM-5 at pulse number 6

hydrogen and the Lewis acid site stabilizes the protonic acid site formed by neutralizing the electron. In fact, almost no isomer products were observed over Ir-free HZSM-5 due to the absence of active sites to generate active protonic acid sites, though HZSM-5 possesses strong Lewis acid sites. Yang and Woo [21] found that Ir/NaY showed higher conversion and stability than Pt/NaY catalyst towards $n$-heptane reforming reaction. They reported that the activity of Ir/NaY catalyst was maintained during the reaction because of the high activity of hydrogenolysis reaction resulting in less amount of coke on the catalyst surface. Finally, it can be concluded that the presence of iridium enhanced the activity and selectivity to *iso*-heptane in $n$-heptane isomerization by facilitating the formation of active protonic acid sites from molecular hydrogen.

## 4. Conclusions

The structural properties studies show that iridium species may interact with structural defect sites through surface OH which stabilizes the crystalline structure of HZSM-5, leading to more ordered framework structure, high surface area and total pore volume of HZSM-5. The interaction between iridium species and surface OH is substantiated by the decrease of the weight loss percentage corresponding to the water content, and the decrease of the hydroxyl group is in the region of $3800-3500\,\mathrm{cm}^{-1}$. The IR studies indicate that iridium species loaded on HZSM-5 slightly increases both protonic and Lewis acid sites without changing the lattice structure of HZSM-5. The Lewis acid sites and iridium, then play an important role in the isomerization of $n$-heptane. Ir/HZSM-5 is found to increase about 4.1%, 33.2% and 11.8% in conversion, selectivity and yield of $n$-heptane isomerization, respectively.

**Acknowledgements**

Our gratitude goes to the Ministry of Science, Technology and Innovation, Malaysia through E-Science Fund Research Project (No. 03-01-06-SF0564 and 03-01-06-SF0289), and the Hitachi Scholarship Foundation for the Gas Chromatograph Instrument Grant.

## References

[1] Ebitani K, Konishi J, Hattori H. *J Catal*, 1991, 130(1): 257
[2] Iglesia E, Soled S L, Kramer G M. *J Catal*. 1993, 144(1): 238
[3] Triwahyono S, Yamada T, Hattori H. *Appl Catal A*, 2003, 242(1): 101
[4] Triwahyono S, Abdullah Z, Jalil A A. *J Nat Gas Chem*, 2006, 15(4): 247
[5] Triwahyono S, Jalil A A, Hattori H. *J Nat Gas Chem*, 2007, 16(3): 252
[6] Demirci Ü B, Garin F. *J Mol Catal A-Chem*, 2007, 271(1-2): 216
[7] Triwahyono S, Jalil A A, Timmiati S N, Ruslan N N, Hattori H. *App Catal A*, 2010, 372(1): 103
[8] Triwahyono S, Yamada T, Hattori H. *Appl Catal A*, 2003, 250(1): 65
[9] Wang W, Wang J H, Chen C L, Xu N P, Mou C Y. *Catal Today*, 2004, 97(4): 307
[10] Nieminen V, Kumar N, Salmi T, Murzin D Y. *Catal Commun*, 2004, 5(1): 15
[11] Fujimoto K, Maeda K, Aimoto K. *Appl Catal A*, 1992, 91(2): 81
[12] Jiménez C, Romero F J, Roldán R, Marinas J M, Gómez J P. *Appl Catal A*, 2003, 249(1): 175
[13] Blomsma E, Martens J A, Jacobs P A. *J Catal*, 1997, 165(2): 241
[14] Cañizares P, de Lucas A, Dorado F, Durán A, Asencio I. *Appl Catal A*, 1998, 169(1): 137
[15] Gault F G, Amir-Ebrahimi V, Garin F, Parayre P, Weisang F. *Bull Soc Chem Belg*, 1979, 88(7-8): 475
[16] Gault F G. *Adv Catal*, 1981, 30: 1
[17] Cañizares P, De Lucas A, Valverde J L, Dorado F. *Ind Eng Chem Res*, 1997, 36(11): 4797
[18] Cañizares P, de Lucas A, Dorado F, Aguirre J. *Microporous Mesoporous Mater*, 2001, 42(2-3): 245
[19] Aboul-Gheit A K, Awadallah A E, Aboul-Gheit N A K, Soly-man E S A, Abdel-Aaty M A. *Appl Catal A*, 2008, 334(1-2): 304
[20] Sinfelt J H. US Patent 3 953 368. 1976
[21] Yang O B, Woo S I. *Stud Surf Sci Catal*, 1993, 75: 671
[22] Triwahyono S, Yamada T, Hattori H. *Catal Lett*, 2003, 85(1-2): 109
[23] Jentys A, Mukti R R, Tanaka H, Lercher J A. *Microporous Mesoporous Mater*, 2006, 90(1-3): 284
[24] Zheng S R, Jentys A, Lercher J A. *J Catal*, 2003, 219(2): 310
[25] Bhavani A G, Karthekayen D, Rao A S, Lingappan N. *Catal Lett*, 2005, 103(1-2): 89
[26] Shen Q, Li L D, Hao Z P, Xu Z P. *Appl Catal B*, 2008, 84(3-4): 734
[27] de Lucas A, Valverde J L, Rodriguez L, Sanchez P, Garcia M T. *Appl Catal A*, 2000, 203(1): 81
[28] M'Ramadj O, Zhang B, Li D, Wang X G, Lu G Z. *J Nat Gas Chem*, 2007, 16(3): 258
[29] Pérez Y O, Forero L A P, Torres D V C, Trujillo C A. *Thermochim Acta*, 2008, 470(1-2): 36
[30] Lercher J A, Jentys A. In: Cejka J, Van Bekkum H, Corma A, Schuth F ed. Introduction to Zeolite Science and Practise, 3rd revised Edition. Amsterdam: Elsevier, 2007. 452
[31] Zecchina A, Geobaldo F, Lamberti C, Bordiga S, Palomino G T, Areán C O. *Catal Lett*, 1996, 42(1-2): 25
[32] Nobukawa T, Sugawara K, Okumura K, Tomishige K, Kunimori K. *Appl Catal B*, 2007, 70(1-4): 342
[33] Guo Q H, Chen B H, Li Y X, Li J W. *Catal Lett*, 2008, 120(1-2): 65
[34] Triwahyono S, Yamada T, Hattori H. *Appl Catal A*, 2003, 250(1): 75
[35] Aboul-Gheit A K, Aboul-Fotouh S M, Aboul-Gheit N A K. *Appl Catal A*, 2005, 283(1-2): 157
[36] Aboul-Gheit A K, Awadallah A E, El-Kossy S M, Mahmoud A L H. *J Nat Gas Chem*, 2008, 17(4): 337
[37] Triwahyono S, Jalil A A, Musthofa M. *Appl Catal A*, 2010, 372(1): 90
[38] Hattori H, Shishido T. *Catal Surv Jpn*, 1997, 1(2): 205